# Inner-electron ionization for wave-packet detection

H. Maeda and T. F. Gallagher
*Department of Physics, University of Virginia, Charlottesville, Virginia 22904*
(Received 14 February 2001; published 11 June 2001)

We describe the use of time-resolved inner-electron ionization as a method of detecting the time evolution of Rydberg wave packets. The method is sufficiently sensitive that it can be used to monitor wave packets for extended times, and its Fourier transform provides a cross correlation between constituent eigenstates, allowing the phases of the constituent eigenstates at the core to be retrieved. These phases, and the easily determined amplitudes of the constituent eigenstates, can be used to construct the wave function of the wave packet.

DOI: 10.1103/PhysRevA.64.013415 PACS number(s): 32.80.Rm, 42.50.Hz, 42.50.Md

## I. INTRODUCTION

Classical motion in atomic and molecular systems can be mimicked using electronic and vibrational quantum wave packets, which are time-dependent coherent superpositions of stationary states [1–3]. For example, a Rydberg radial electronic wave packet $\Psi(r,t)$ can be written as

$$\Psi(r,t)=\sum_j a_j\psi_j(r)\exp[-i(W_jt-\phi_j)], \qquad (1)$$

where $\psi_j(r)$ is the radial wave function of the $j$th composite eigenstate of the wave packet, $W_j$ its energy, $\phi_j$ its phase, and the amplitude $a_j$ is real and positive, where $\Sigma_j a_j^2=1$. The angular part of each of the stationary-state wave functions is constant and the same for all $j$, so we ignore it.

For radial Rydberg wave packets of many-electron atoms such as alkali and alkaline-earth atoms, the eigenenergies $W_j$ of the composite states are accurately known, and it is straightforward to determine the amplitudes $a_j$ by using state-selective field ionization (SSFI) [4]. Determining the phase $\phi_j$ is, however, more challenging. In general, it requires a cross correlation between different constituent eigenstates, and the most straightforward approach is to use time-resolved detection. It is possible, however, to use interferometry between the unknown wave packet and a known reference wave packet [5]. Unfortunately, the simple approach of interferometry using two identical wave packets, the optical Ramsey method [6,7], does not give a cross correlation. As noted above, the most general approach to phase retrieval is to use time-resolved detection. Time-resolved detection with isolated core excitation [8] and half-cycle pulses (HCP's) [9,10] has been reported, and the relative phase of the constituent eigenstates has been determined [11]. It has also been demonstrated that time-resolved measurement with an atomic streak camera [12] provides the relative phase information of a Stark wave packet in the vicinity of a saddle point [13]. Recently, a terahertz HCP, together with SSFI, has been used to retrieve phase information stored in sculpted Rydberg wave packets [14]. Here we report an alternative method of time-resolved detection for phase retrieval, inner-electron ionization (IEI) [15,16]. The method can be thought of as a variant of photoionization detection [17,18]. Like photoionization detection, frequency chirp or related laser-pulse characteristics are unlikely to introduce differences in the detection efficiency for different constituent states of the wave packet. However, our method is substantially more efficient than photoionization detection, allowing wave packets to be monitored for longer times [19].

In this paper, we first review the basic notions of IEI for wave packet detection and provide a model for the process in Sec. II. In Sec. III, our experimental approach is described. Finally, in Sec. IV, we present typical data for Sr $5snd\,^1D_2$ wave packets, extract the relative phases $\phi_j$ by analyzing our results, and compare the synthesized wave-packet signals from the extracted amplitudes and phases to the observed signals.

## II. INNER-ELECTRON IONIZATION OF A RYDBERG WAVE PACKET

The general notion behind IEI is easily understood by referring to the Sr energy level diagram of Fig. 1 [20,21]. In our experiment, Sr is excited from the ground $5s^2\,^1S_0$ state to the $5s6p\,^1P_1$ state by a frequency doubled 586-nm, 5-ns dye laser pulse. Atoms in the $5s6p\,^1P_1$ state are excited to a $5snd\,^1D_2$ wave packet by a pulse obtained from a 230-fs Titanium:sapphire ($Ti:Al_2O_3$) laser operated at 854 nm. After a variable delay time, the atoms are exposed to a 427-nm pulse obtained by frequency doubling the 854-nm $Ti:Al_2O_3$ laser pulse. To understand the effect of the 427-nm pulse on a Sr $5snd$ atom, it is useful to think of the atom as a $Sr^+$ ion and an outer $nd$ electron. The 427-nm pulse is nearly resonant with the $Sr^+$ $5s-5p$ and $5p-6s$ transitions at 422 and 416 nm. Therefore, the $Sr^+$ $5s$ ion can be efficiently photoionized to produce $Sr^{++}$ by absorbing four photons of the 427-nm light pulse. Consequently, if a Sr $5snd$ atom is exposed to the 427-nm pulse, the $5s$ electron can be ejected from the atom by multiphoton ionization. If the outer $nd$ electron is at or near its outer classical turning point when the $Sr^+$ $5s$ electron is ejected, the outer electron is projected from a Sr $5snd$ state onto $Sr^+$ $n'd$ Rydberg states with $n'\sim\sqrt{2}n$. On the other hand, if the outer electron is near its inner turning point, the $5s$ electron can not be ejected without disturbing the $nd$ electron, and no $Sr^+$ Rydberg ions are produced. Detection of $Sr^+$ Rydberg ions indicates that the outer electron was far from the ionic core when the 427-nm pulse arrived, and by scanning the delay of the 427-nm laser pulse relative to the 854-nm pulse we can detect the time-dependent motion of the Rydberg electron wave packet [19].

 

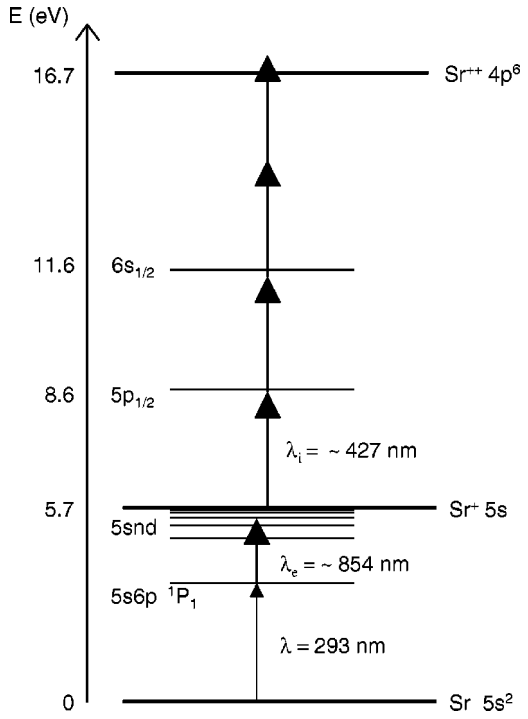


FIG. 1. Energy level of Sr, showing the excitation of the Sr $5snd$ wave packet by the first two laser pulses at 293 nm and 854 nm. After the variable delay $t$ ($<250$ ps), the third laser pulse at 427 nm multiphoton ionizes the $Sr^+$ $5s$ core electron.

It is straightforward to construct a model of the detection of the time evolution of the wave packet. We assume that the IEI signal $S(t)$ at time delay $t$ between the 854- and 427-nm pulses is given by

$$S(t)=\alpha P_{MPI}[1-\overline{P}(t)], \tag{2}$$

where $\alpha$ represents a normalization factor, $P_{MPI}$ is the multiphoton ionization probability of $Sr^+$ by the 427-nm pulse, and $\overline{P}(t)$ is the probability of finding the outer $nd$ electron near the inner core, i.e., at small $r$ during the 427-nm pulse. At small $r$, the radial wave function $\psi_j(r)$ is given by

$$\psi_j(r)=\nu_j^{-3/2}f(r), \tag{3}$$

where the effective quantum number $\nu_j$ is defined by $W_j=-1/2\nu_j^2$ in atomic units (a.u.) [22]. Using Eq. (3), we can write the probability $P(t)$ of finding the $nd$ electron near the core at time $t$ as

$$\begin{aligned}P(t)&=\int_0^R\left|\sum_j a_j\nu_j^{-3/2}f(r)\exp[-i(W_jt-\phi_j)]\right|^2r^2dr\\&=\Gamma\left[\sum_j \nu_j^{-3}a_j^2+2\sum_{j,k>j}(\nu_j\nu_k)^{-3/2}a_ja_k\right.\\&\quad\left.\times\cos(W_{kj}t-\phi_{kj})\right],\end{aligned} \tag{4}$$

where

$$\Gamma=\int_0^R f(r)^2r^2dr, \tag{5}$$

in which $R$ is the radius that defines ''small $r$'' or ''near the core,'' $W_{kj}=W_k-W_j$, and $\phi_{kj}=\phi_k-\phi_j$, respectively.

To allow for the finite temporal width of the laser pulse, assumed Gaussian, we average $P(t)$ over the laser pulse duration, i.e.,

$$\overline{P}(t)=\frac{\Gamma\int_{-\infty}^{\infty}\exp\left(-\ln 2\frac{t'^2}{T^2}\right)P(t-t')dt'}{\int_{-\infty}^{\infty}\exp\left(-\ln 2\frac{t'^2}{T^2}\right)dt'}, \tag{6}$$

where $T$ is the half width at half maximum of the Gaussian pulse duration. Carrying out the integral yields

$$\begin{aligned}\overline{P}(t)=\Gamma\left[\sum_j \nu_j^{-3}a_j^2+2\sum_{j,k>j}(\nu_j\nu_k)^{-3/2}a_ja_k\right.\\\left.\times\cos(-W_{kj}t+\phi_{kj})\exp\left(-\frac{W_{kj}^2T^2}{4\ln 2}\right)\right].\end{aligned} \tag{7}$$

Combining Eqs. (2) and (7) gives a compact description of IEI. Of the parameters in Eq. (7), the spectroscopic values $\nu_{kj}$ and $W_{kj}$ can be determined using the quantum defect $\delta_d$ of the Sr $5snd\ ^1D_2$ states, given by $\delta_d=2.30$. The values of $a_j$ can be deduced experimentally by SSFI. As we shall show, it is possible to determine the relative values of $\phi_{kj}$ at the core by Fourier analyzing the time-dependent IEI signal and to reconstruct the wave function of the wave packet.

## III. EXPERIMENTAL METHODS

The fs laser system consists of a continuous-wave, mode-locked $Ti:Al_2O_3$ laser that is amplified by a regenerative amplifier running at a 20-Hz repetition rate to produce 2-mJ, 230-fs pulses when operated at 854 nm. Each pulse is split in two by a beam splitter. The ionization pulse at 427 nm is produced by frequency doubling one of the split 854-nm pulses by a 0.5-mm-long beta-barium borate (BBO) (Type I) crystal, and its angle is set so as to maximize the IEI signal. This 427-nm light is tightly focused by a 50-cm focal length lens, and the peak intensity is estimated to be approximately $8\times10^{12}$ W/cm$^2$ at the focal point. On the other hand, the excitation laser at 854 nm, whose energy when it reaches the interaction region is 150 $\mu$J per pulse and only weakly focused with a 2-m focal length lens, is directed into a set of polarizers to control its polarization. The polarizers reduce the effective bandwidth of 854-nm light to approximately 40 cm$^{-1}$. This pulse excites Sr in the $5s6p\ ^1P_1$ intermediate state, producing predominantly a Sr $5snd$ wave packet with an average effective quantum number $\overline{\nu}$, which can be varied over the range $25\leqslant\overline{\nu}\leqslant35$ by slightly tuning the wavelength of the $Ti:Al_2O_3$ laser. The relative time delay between the two pulses is varied, up to 250 ps, by moving a roof prism on a mechanical translation stage in the excitation laser path.

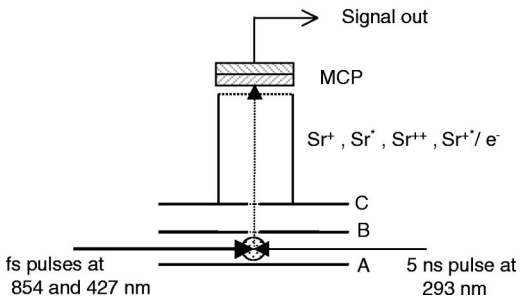


FIG. 2. Diagram of the interaction region. We detect ions to monitor the time evolution of the wave packets, whereas electrons are detected when the squared amplitudes $a_j^2$ of the constituent states of the wave packets are measured by SSFI.

Both fs pulses are recombined in front of the vacuum chamber with a dichroic mirror and collinerly introduced into it. From the opposite side of the chamber, the 586-nm, 5-ns dye-laser pulse is introduced counter propagating to the fs pulses, and all three laser beams intersect the Sr effusive atomic beam at nearly a right angle between a pair of capacitor plates separated by 0.3 cm, as shown by Fig. 2. Approximately 100 ns after the interaction of the laser pulses with the atoms, an adjustable positive pulsed voltage (0–9 kV) of 1-$\mu$s rise time is applied to the bottom plate, *A* in Fig. 2, to field-ionize the $Sr^+$ Rydberg ions due to IEI. The same field pushes all ions produced between the capacitor plates out of the interaction region via a mesh in the upper plate, *B* in Fig. 2, into a second field region defined by plate *B* and a third field plate, *C* in Fig. 2. After leaving the second field region, the ions pass through a field-free region, inside the metal tube attached to plate *C*, on their way to the microchannel plate (MCP) detector. We apply an adjustable constant voltage (typically a few hundred volts) to the plate *C* so as to achieve the optimum time resolution of the signal. We distinguish signals resulting from field-ionized Sr Rydberg atoms, multiphoton-ionized $Sr^+$, field-ionized $Sr^+$ Rydberg ions, and multiphoton-ionized $Sr^{2+}$, which we denote Sr*, $Sr^+$, $Sr^+$*, and $Sr^{2+}$, respectively, by their different times-of-flight (TOF), as shown in Fig. 3.

In addition to monitoring the time evolution of the wave packet, we can separately measure the squared amplitude $a_j^2$ of each of the constituent $5snd\,^1D_2$ states of the wave packet using SSFI. In this case, we apply a 1-$\mu$s-rise time, negative-pulsed voltage instead of the positive pulse to the bottom plate *A* of the capacitor plates defining the interaction region and detect electrons with the MCP. Plates *B* and *C* are grounded. Electrons are ejected from each state in the wave packet when the strength of the ramped field between the plates reaches its classical field-ionization threshold. Since the flight time of the electrons is negligible, the time dependence of the SSFI signal gives directly the squared amplitudes or populations in the eigenstates constituting the wave packet.

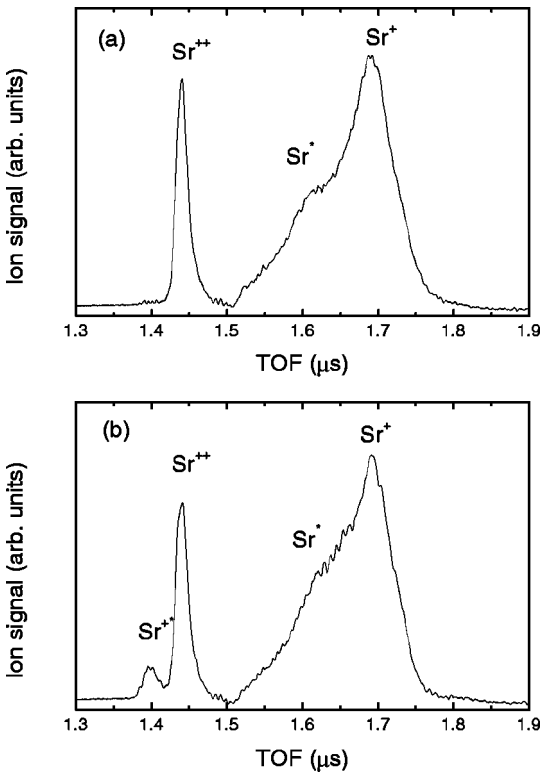


FIG. 3. Typical TOF ionization spectra of Sr taken (a) at the delay time $t<0$, and (b) at $t>0$. It is obvious the $Sr^+$* signal appears significantly only at $t>0$.

## IV. RESULTS

In Fig. 4(a) we show a typical IEI spectrum obtained by setting a boxcar gate on the $Sr^+$* signal and scanning the time-delay *t* between the 854- and 427-nm pulses. As shown, there are just a few recurrences at integer multiples of the recurrence time, $\tau_{rc}\sim 2.9$ ps, before the clear oscillations in the signal almost disappear. From these recurrences alone it would be almost impossible to determine a good value of $\tau_{rc}$. Fortunately, the oscillating structure reappears at the

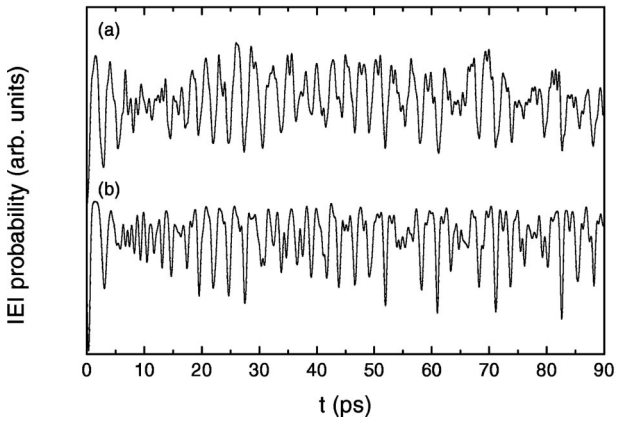


FIG. 4. The IEI signal from a Sr $5snd$ wave packet with $\bar{\nu}=26.4$ plotted against the delay *t*; (a) the experimentally measured $Sr^+$* field-ionization signal, and (b) the IEI signal calculated using Eq. (2) (see text, for details).

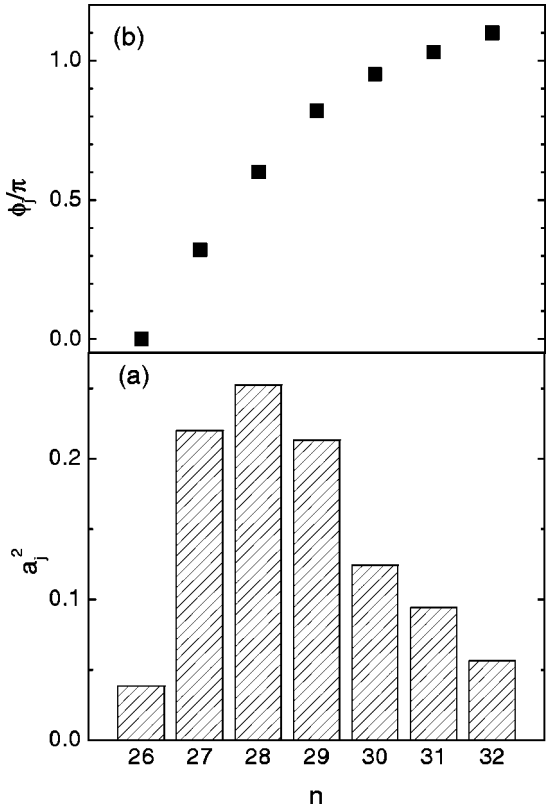


FIG. 5. Measured squared amplitudes $a_j^2$ and phases $\phi_j$ of the constituent states of the Sr $5snd$ wave packet of $\bar{\nu}=26.4$ shown in Fig. 4(a); (a) $a_j^2$ determined from the SSFI measurement, and (b) $\phi_j$ retrieved from the Fourier transform of the time-dependent signal in Fig. 4(a). Note that we have set the phase of the $n=26$ state to zero as only phase differences $\phi_{kj}$ can be recovered by Fourier transform of the time-dependent IEI signal.

revivals, at integral multiples of the revival time, $\tau_{rv}$ $\sim 24.6$ ps. Note that the revivals occur exactly at half integral multiples of $\tau_{rc}$ in odd revivals, and at an integer multiples of $\tau_{rc}$ in even revivals, which is a consequence of our definitions of $\tau_{rc}$ and $\tau_{rv}$, as described in detail in the Appendix.

As mentioned in Sec. II, in our model the time-dependent IEI signal depends on the constituent states' spectroscopic parameters $\nu_j$ and $W_j$, and the amplitudes $a_j$ and phases $\phi_j$ of the wave packet. To reconstruct the wave packet, we need to derive information on both $a_j$ and $\phi_j$ from the experimental measurements. The amplitudes $a_j$ can be obtained from time-resolved SSFI signals of the wave packet, which give peaks with areas proportional to $a_j^2$ for each states. In Fig. 5(a) we plot values of $a_j^2$ of the wave packet whose time-dependent IEI signal is given in Fig. 4(a). It has been demonstrated recently by Jones and Campbell that, to within an overall phase, the phases $\phi_j$ of the constituent states can be obtained from the Fourier transform of the time-dependent probability of finding the wave packet in a small volume [11]. As described in Sec. II, since the IEI signal reflects the time-dependent probability of finding the wave packet at the core, it is possible to perform a Fourier transform of the trace in Fig. 4(a) to extract the phases $\phi_j$ of the constituent states.

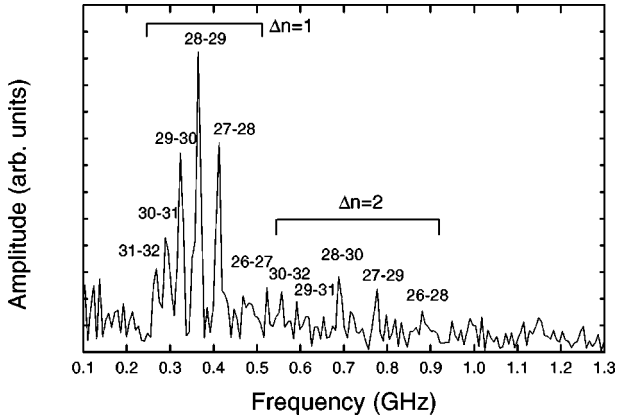


FIG. 6. Discrete Fourier transform of the time-dependent IEI signal shown in Fig. 4(a). Note that the frequency components from the states differing in $n$ by three or more are barely visible, so these peaks are not labeled in the figure.

Given in Fig. 6 is a plot of the Fourier transform of the IEI signal in Fig. 4(a). As shown, the frequency components from composite states differing in $n$ by one are quite evident, but the components corresponding to states differing in $n$ by two are less evident and by three or more are at best barely visible. Thus, we deduced the phase difference $\phi_{kj}$ from the $\Delta n=1$ components in Fig. 6. It is useful to note that the phase variation has two contributions. First, $\phi_j$ changes monotonically with $j$ as the point defined as $t=0$ in the analysis is moved relative to the time of the exciting laser pulse. This change in $\phi_j$ has no physical content, it merely allows us to shift the time scale. Second, there is a variation in $\phi_j$ due to the chirp, etc., in the excitation process. Using our freedom to choose the overall phase of the wave function, we have set the phase of the $n=26$ state to zero. The resulting phases $\phi_j$ of the constituent states are plotted in Fig. 5(b).

The most straightforward test of how well we have characterized the wave packet is to use the amplitudes and phases extracted from the data set, together with parameters $\nu_j$ and $W_j$, to reproduce the IEI signal shown in Fig. 4(a). In this case, we calculated time-dependent IEI signal using Eq. (2) to achieve a nonlinear least-square fit to the experimental data in Fig. 4(a) by adjusting the parameters $A=\alpha P_{MPI}$ [see Eq. (2)], $\Gamma$ [see Eq. (7)], and an additional parameter to compensate for the background offset in the signal. In Fig. 4(b), we show the calculated results. The overall agreement between the experimental and calculated signals is reasonable. Note that we use in this calculation the value of $T=200$ fs. Thus $2T$, the full width at half maximum is nearly 1.7 times as long as the pulse width of the fundamental light at 854 nm. A possible cause of the pulse broadening of the frequency-doubled light might be the slight phase mismatch in the second harmonic generation by the BBO crystal.

From the calculation mentioned above, a value of $\Gamma=0.013$ is obtained. With this value of $\Gamma$, by using Eq. (5), and approximating the radial wave function $\psi$ in Eq. (3) by a hydrogenic wave function, we can estimate the size of $R$, which defines the small $r$ region in which photoionization of the radial wave packet mainly occurs, as 1.8 a.u. This value

is reasonably close to the radius of the $Sr^+$ $5s_{1/2}$ core, 2.5 a.u., supporting the validity of our simple model.

## V. SUMMARY

In summary, we have demonstrated that IEI can be used as an effective method for detecting the radial Rydberg wave packets in two- or many-electron atoms. As the IEI signal reflects the time-dependent probability of the wave packet's being at the core for long times, phase information for the constituent states can be retrieved by a Fourier transform of the time-dependent IEI signal. Combining the phases from IEI and the amplitudes from SSFI can define the quantum wave function of the Rydberg wave packet, which is crucial for the control of the quantum dynamics.

## ACKNOWLEDGMENTS

The authors would like to thank R.R. Jones for many insights into this subject. We also thank W. Li for experimental assistance. This work is supported by the U.S. Department of Energy.

## APPENDIX: EFFECTS OF NONINTEGRAL VALUE OF $\bar{\nu}$ ON $\tau_{rc}$ AND $\tau_{rv}$

As mentioned in Sec. I, a nonstationary radial Rydberg wave packet is a coherent superposition of stationary Rydberg eigenstates, and ignoring the constant angular parts of the wave function, we can express its wave function $\Psi$ by Eq. (1) of Sec. I. The temporal periodicity of the wave packet, which resembles the classical motion of the atomic electron, is determined by the time varying phase factors $\exp(-iW_jt)$, i.e., by the energies $W_j$ of the constituent eigenstates. To show the quantum-classical connection most clearly, it is useful to expand the energies of the constituent states around the average energy of the wave packet. This procedure has been used by several authors, beginning with Averbukh and Perelman [23]. Usually the expansions are done for hydrogen energies with the additional assumption that the average energy coincides with that of a hydrogenic level. Wals *et al.* extended the analysis to include either nonhydrogenic energy levels or a nonhydrogenic average energy, but not both simultaneously [24]. Here we present a general development that shows that the latter two effects enter in the same way. A similar conclusion was reached by Bluhm and Kostelecký using a supersymmetry-based quantum-defect theory [25].

The energy $W_j$ of a Rydberg eigenstate of a nonhydrogenic atom is given as

$$W_j=-\frac{1}{2\nu_j^2}=-\frac{1}{2(n_j-\delta)^2}, \tag{A1}$$

where $\nu_j$ is the effective quantum number, $\delta$ is the constant quantum defect of the Rydberg series, and $n_j$ is an integral principal quantum number. Atomic units are used throughout the Appendix. The average energy of the wave-packet $\bar{W}$, determined by the tuning of the exciting laser, is

$$\bar{W}=-\frac{1}{2\bar{\nu}^2}=-\frac{1}{2(\bar{n}-\bar{\delta})^2}, \tag{A2}$$

where $\bar{n}$ is an integer but $\bar{\nu}$ is not, in general. Here $\bar{\delta}$ reflects how far the average energy lies from a hydrogenic energy.

The energy $W_j$ of each constituent state of the wave packet can be expressed as a Taylor series in $\bar{\nu}$ about $\bar{W}$,

$$W_j=\bar{W}+\left.\frac{d\bar{W}}{d\nu}\right|_{\bar{\nu}}\Delta\nu_j+\frac{1}{2}\left.\frac{d^2\bar{W}}{d\nu^2}\right|_{\bar{\nu}}(\Delta\nu_j)^2+\cdots, \tag{A3}$$

where $\Delta\nu_j=\nu_j-\bar{\nu}$. For any eigenstate in the wave packet, the energy to second order in $\Delta\nu_j$ is given by

$$W_j=-\frac{1}{2\bar{\nu}^2}+\frac{(\nu_j-\bar{\nu})}{\bar{\nu}^3}-\frac{3}{2}\frac{(\nu_j-\bar{\nu})^2}{\bar{\nu}^4}. \tag{A4}$$

Setting

$$\nu_j-\bar{\nu}=\Xi+\xi \tag{A5}$$

where $\Xi=n_j-\bar{n}$ is an integer (different for each state $j$), and $\xi=\bar{\delta}-\delta$, defined modulo 1 such that $|\xi|<1/2$, we can rewrite the phase factor as

$$\exp(-iW_jt)=\exp[-i(A+B+C)t], \tag{A6}$$

where

$$A=-\frac{1}{2\bar{\nu}^2}+\frac{\xi}{\bar{\nu}^3}-\frac{3\xi^2}{2\bar{\nu}^4}, \tag{A7}$$

$$B=\frac{1}{\bar{\nu}^3}\left(1-\frac{3\xi}{\bar{\nu}}\right)\Xi, \tag{A8}$$

and

$$C=-\frac{3}{2\bar{\nu}^4}\Xi^2, \tag{A9}$$

respectively. The term $A$ gives a very rapidly varying phase common to all states, which is unimportant. The second term $B$, proportional to $\Xi$, gives a rapidly varying phase factor, which is equal to one for all $j$ states at the recurrence time $\tau_{rc}$, i.e., when

$$\frac{1}{\bar{\nu}^3}\left(1-\frac{3\xi}{\bar{\nu}}\right)\Xi\ \tau_{rc}=2\pi N, \tag{A10}$$

where $N$ is an integer. Consequently we define the recurrence time $\tau_{rc}$ as

$$\tau_{rc}=2\pi\bar{\nu}^3\left(1-\frac{3\xi}{\bar{\nu}}\right)^{-1}, \tag{A11}$$

which is slightly different from the usual classical recurrence time $\tau_{cl}=2\pi\overline{\nu^3}$. The third term $C$ proportional to $\Xi^2$, gives a slowly varying phase factor and determines the revival time. It is defined by Averbukh and Perelman [23] as the time when this contribution to the phase factor is equal to one for all states, i.e.,

$$\frac{3}{2\overline{\nu^4}}\Xi^2\tau_{AP}=2\pi N \tag{A12}$$

for all $\Xi$, giving a revival time of

$$\tau_{AP}=\frac{4\pi\overline{\nu^4}}{3}. \tag{A13}$$

The more common definition of the revival time [1,26] is obtained by setting

$$\frac{3}{2\overline{\nu^4}}\Xi^2\tau_{rv}=\pi N, \tag{A14}$$

yielding

$$\tau_{rv}=\frac{2\pi\overline{\nu^4}}{3}=\frac{\overline{\nu}}{3}\tau_{cl}. \tag{A15}$$

With our definition of $\tau_{rc}$ the full revivals in the wave-packet signals are always observed at integer or half integer values of $\tau_{rc}$. In contrast, it is only true that the signals occur at integer and half integer values of $\tau_{cl}$ if $\xi=0$, which only occurs when the average energy $\overline{W}$ of the wave packet coincides with the energy $W_j$ of one of the constituent eigenstates. Such a coincidence only occurs by chance, even in hydrogen.

It is apparent that if the energy is expanded to higher order in $\nu_j-\overline{\nu}$, the values of $\tau_{rc}$ and $\tau_{rv}$ change slightly. For example, adding one more term to the energy expansion in Eq. (A4) leads to

$$\tau_{rc}=\tau_{cl}\left(1-\frac{3\xi}{\overline{\nu}}+\frac{6\xi^2}{\overline{\nu^2}}\right)^{-1} \tag{A16}$$

and

$$\tau_{rv}=\tau_{cl}\frac{\overline{\nu}}{3}\left(1-\frac{4\xi}{\overline{\nu}}\right)^{-1}. \tag{A17}$$


[1] J. Parker and C.R. Stroud, Jr., Phys. Rev. Lett. **56**, 716 (1986).
[2] G. Alber, H. Ritsch, and P. Zoller, Phys. Rev. A **34**, 1058 (1986).
[3] M.J. Rosker, T.S. Rose, and A.H. Zewail, Chem. Phys. Lett. **146**, 175 (1988).
[4] T.F. Gallagher, L.M. Humphrey, W.E. Cooke, R.M. Hill, and S.A. Edelstein, Phys. Rev. A **16**, 1098 (1977).
[5] T.C. Weinacht, J. Ahn, and P.H. Bucksbaum, Phys. Rev. Lett. **80**, 5508 (1998); T.C. Weinacht, J. Ahn, and P.H. Bucksbaum, *ibid.* **81**, 3050 (1998).
[6] L.D. Noordam, D.I. Duncan, and T.F. Gallagher, Phys. Rev. A **45**, 4734 (1992).
[7] R.R. Jones, C.S. Raman, D.W. Schumacher, and P.H. Bucksbaum, Phys. Rev. Lett. **71**, 2575 (1993).
[8] R.R. Jones, Phys. Rev. A **57**, 446 (1998).
[9] C. Raman, C.W.S. Conover, C.I. Sukenik, and P.H. Bucksbaum, Phys. Rev. Lett. **76**, 2436 (1996).
[10] R.R. Jones, Phys. Rev. Lett. **76**, 3927 (1996).
[11] R.R. Jones and M.B. Campbell, Phys. Rev. A **61**, 013403 (1999).
[12] G.M. Lankhuijzen and L.D. Noordam, Phys. Rev. Lett. **76**, 1784 (1996).
[13] C.W. Rella, F. Texier, L.D. Noordam, and F. Robisheaux, Phys. Rev. Lett. **85**, 4233 (2000).
[14] J. Ahn, D.N. Hutchinson, C. Rangan, and P.H. Bucksbaum, Phys. Rev. Lett. **86**, 1179 (2001).
[15] R.R. Jones and P.H. Bucksbaum, Phys. Rev. Lett. **67**, 3215 (1991).
[16] H. Stapelfeldt, D.G. Papaiouannou, L.D. Noordam, and T.F. Gallagher, Phys. Rev. Lett. **67**, 3223 (1991).
[17] A. ten Wolde, L.D. Noordam, A. Lagendijk, and H.B. van Linden van den Heuvell, Phys. Rev. Lett. **61**, 2099 (1988).
[18] J.A. Yeazell, M. Mallalieu, J. Parker, and C.R. Stroud, Jr., Phys. Rev. A **40**, 5040 (1989).
[19] H. Maeda, W. Li, and T.F. Gallagher, Phys. Rev. Lett. **85**, 5078 (2000).
[20] C.E. Moore, in *Atomic Energy Levels*, Natl. Bur. Stand. (U.S.) Circ. No. 467 (U.S. GPO, Washington, DC, 1958), Vol. II, p. 189.
[21] P. Esherick, Phys. Rev. A **15**, 1920 (1977).
[22] H.A. Bethe and E.E. Salpeter, *Quantum Mechanics of One- and Two-Electron Atoms* (Plenum, New York, 1977).
[23] I.Sh. Averbukh and N.F. Perelman, Phys. Lett. A **139**, 449 (1989).
[24] J. Wals, H.H. Fielding, and H.B. van Linden van den Heuvell, Phys. Scr., T **58**, 62 (1995).
[25] R. Bluhm and V.A. Kostelecký, Phys. Rev. A **50**, R4445 (1994).
[26] J.A. Yeazell, M. Mallalieu, and C.R. Stroud, Jr., Phys. Rev. Lett. **64**, 2007 (1990).